Plant, Cell & Environment

Plant, Cell and Environment (2016) doi: 10.1111/pce.12688

Original Article

Grapevine petioles are more sensitive to drought induced embolism than stems: evidence from *in vivo* MRI and microcomputed tomography observations of hydraulic vulnerability segmentation

Uri Hochberg[1,2], Caetano Albuquerque[3], Shimon Rachmilevitch[4], Herve Cochard[2], Rakefet David-Schwartz[5], Craig R. Brodersen[6], Andrew McElrone[3,7] & Carel W. Windt[8]

[1]Dipartimento di Scienze Agrarie e Ambientali, University of Udine, 33100 Udine, Italy, [2]INRA, UMR 547 PIAF/Université Blaise Pascal, F-63039 Clermont-Ferrand, France, [3]Department of Viticulture and Enology, University of California, Davis, CA 95616, USA, [4]The Jacob Blaustein Institute for Desert Research, Ben-Gurion University of the Negev, Be'er Sheva 84990, Israel, [5]Institute of Plant Sciences, Agricultural Research Organization, The Volcani Centre, Bet Dagan 50250, Israel, [6]School of Forestry and Environmental StudiesYale UniversityNew Haven, CT 06511, USA, [7]Crops Pathology and Genetics Research Unit, USDA-ARS, Davis, CA 95616, USA and [8]Forschungszentrum Jülich, Institute for Bio- and Geosciences, IBG-2: Plant Sciences, 52425 Jülich, Germany

ABSTRACT

The 'hydraulic vulnerability segmentation' hypothesis predicts that expendable distal organs are more susceptible to water stress-induced embolism than the main stem of the plant. In the current work, we present the first *in vivo* visualization of this phenomenon. In two separate experiments, using magnetic resonance imaging or synchrotron-based microcomputed tomography, grapevines (*Vitis vinifera*) were dehydrated while simultaneously scanning the main stems and petioles for the occurrence of emboli at different xylem pressures (Ψ_x). Magnetic resonance imaging revealed that 50% of the conductive xylem area of the petioles was embolized at a Ψ_x of −1.54 MPa, whereas the stems did not reach similar losses until −1.9 MPa. Microcomputed tomography confirmed these findings, showing that approximately half the vessels in the petioles were embolized at a Ψ_x of −1.6 MPa, whereas only few were embolized in the stems. Petioles were shown to be more resistant to water stress-induced embolism than previously measured with invasive hydraulic methods. The results provide the first direct evidence for the hydraulic vulnerability segmentation hypothesis and highlight its importance in grapevine responses to severe water stress. Additionally, these data suggest that air entry through the petiole into the stem is unlikely in grapevines during drought.

Key-words: cavitation; hydraulic conductance; *Vitis vinifera*; xylem; vulnerability curves.

INTRODUCTION

Water flows through xylem conduits at negative pressures (i.e. tension) that can be well below vapour pressure. Under such tensions, water is in a metastable state (Dixon 1914) and at risk of cavitation that results in subsequent loss of function in the conduit (Tyree & Sperry 1989). The concept of 'plant segmentation' was introduced over 30 years ago (Zimmermann 1983) and proposes that hydraulic constraints enable the plant to sacrifice organs of lesser importance and investment in order to save organs that are critical for long-term survival and propagation. Zimmerman (1983) suggested 'hydraulic segmentation' as a mechanism in which high resistance results in a high gradient of xylem pressure between the basal and distal plant parts. Eight years later, Tyree & Ewers (1991) coined the term 'vulnerability segmentation', suggesting a second mechanism in which expendable organs (e.g. leaves) in woody plants are more susceptible to embolism, compared with more permanent structures. Supporting this idea, cavitation vulnerability curves of petioles and stems in walnut trees (*Juglans regia* L.) showed that petioles are significantly more susceptible than stems; petioles lost 50% of their hydraulic conductivity at xylem pressures ($\Psi_{50\%}$) of −1.5 MPa, as compared with −2.2 MPa in stems (Tyree *et al.* 1993). Similarly, Tsuda & Tyree (1997) reported $\Psi_{50\%}$ of −2.0 and −0.5 MPa for stems and petioles, respectively. Choat *et al.* (2005) have even shown that in sugar maple trees (*Acer saccharum* Marsh.), the increase in air seeding threshold of different organs is a function of their distance from the trunk. While this pattern has been documented in some species, the opposite was found in others (i.e. stems more susceptible than leaves; Cochard *et al.* 1992), suggesting that the phenomenon is not universal across species.

A comparison of vulnerability curves collected by different research groups suggests that grapevines (*Vitis vinifera* L.) belong to the group of species that do exhibit vulnerability segmentation, with stems that are more resistant to water stress-induced embolism than the petioles (Alsina *et al.* 2007; Choat *et al.* 2010; Zufferey *et al.* 2011; Tombesi *et al.* 2014). A comparison of acoustic emissions in detached stems and petioles of Syrah and Grenache vines revealed that most of the

Correspondence: U. Hochberg; e-mail: uriho9842@yahoo.com;

petiole vessels embolized at a xylem pressure (Ψ_x) of −1.5 MPa, whereas the formation of emboli was still occurring in the stem at Ψ_x as low as −2 MPa (Schultz 2003). A comparison performed by Lovisolo *et al.* (2008) of embolism in different organs of water-stressed grapevines showed that at $\Psi_x = -1.4$ MPa, 80% loss of conductance (PLC) was measured in the petioles, whereas the stems exhibited only 45% PLC. These lines of evidence suggest that there is a high probability for vulnerability segmentation in grapevines (Zufferey *et al.* 2011), although this hypothesis has yet to be explicitly tested. Furthermore, the debate about the validity of previous measurements of embolism (Cochard, Delzon & Badel 2015) calls for a direct measurement and observation of the phenomenon *in vivo*.

Over the last 5 years, the validity of previous embolism measurements in long vessel species, such as grapevines, has been questioned. It appears that measurements of some species with a large population of long vessels (i.e. longer than the length of the sample) are prone to a bias when the centrifuge technique is used or when cutting stem samples under tension (even when under water; Choat *et al.* 2010; Wheeler *et al.* 2013; Torres-Ruiz *et al.* 2015), calling for non-invasive methods to measure or visualize the formation and spread of emboli *in vivo*. Magnetic resonance imaging (MRI) and X-ray microcomputed tomography (microCT) have been successfully used to visualize embolism formation in a number of studies (Holbrook *et al.* 2001; Scheenen *et al.* 2007; Choat *et al.* 2010; Zwieniecki, Brodersen *et al.* 2010; Brodersen *et al.* 2013; Melcher & Ahrens 2013; Knipfer *et al.* 2014).

In the current study, we used MRI and microCT as complementary diagnostic imaging tools to evaluate embolism formation in stems and petioles while they are still connected to one another. Both imaging techniques were used to test the vulnerability segmentation hypothesis independently and to validate previous indirect measurements of grapevine petiole vulnerability curves.

MATERIALS AND METHODS

This study consisted of two separate experiments. Both compared the occurrence of xylem emboli in the petioles and stems of drying grapevines. In the first experiment, four plants were disconnected from their root system by cutting the rootstock and subjected to fast dehydration for a time period of between 12 and 40 h, while continuously monitoring events of embolism formation by MRI. To acquire improved spatial resolution images of the phenomenon and to validate that results were not affected by cutting the rootstock, a second experiment utilized synchrotron-based microCT technology to observe the same phenomenon. Intact plants were dried to the $\Psi_{50\%}$ that was observed in the MRI experiment and then imaged.

Plant material

The MRI experiment was conducted on 1-year-old Syrah vines grafted on SO4 rootstocks, grown in commercial potting soil (Einheitserde Classic, type ED73) in 10 L pots. During the 65–85 days growth period, between budbreak and the imaging, the vines were grown in a growth chamber at 24 °C and 80% relative humidity. Artificial lighting of 300 μmol m^{-2} s^{-1} photosynthetic photo flux density with 14/10 day/night cycles was used. The vines were pruned to yield a single long stem without side branches to fit the bore of the MRI imager and were approximately 2.5 m long and had between 15 and 19 leaves at the time of imaging. Irrigation to soil saturation was applied daily prior to imaging. Random sampling of the xylem water pressure with a pressure chamber was carried out to ascertain that vines were maintained at a xylem pressure higher than −0.5 MPa.

The four plants utilized in the microCT experiment were own-rooted Syrah grapevines donated by the Foundation Plant Services (Davis, CA, USA) and grown in 0.5 L pots containing a potting mix (Berger BM-6- with a composition of mostly dolomite, perlite, peat moss and micronutrients) in a UC Davis glasshouse facility. The plants were in their first year, 8 weeks after budburst. All samples were maintained in a well-watered condition prior to use in the experiment and received 10% Hoagland solution twice a day. Watering for the drought-stressed plants was ceased approximately 1 week prior to the experiment, and the pots dried down slowly over this time. Samples were transported to the Advanced Light Source at the Lawrence Berkeley National Lab, Berkeley, CA, USA on the same day of microCT scanning.

Preparation and installation of the vines in the magnetic resonance imaging scanner

The MRI experiment was designed to image embolism formation in fast drying xylem with no open vessels in the imaged area. To study the maximal vessel length originating from the rootstock, we followed the procedure described by Ewers & Fisher (1989). Plants were cut in the middle of the rootstock, and air was forced at 200 kPa into the open cut. The apical part of the stem was immersed in water and progressively cut back in 2 cm intervals until bubbles were observed escaping the cut surface. This method verified that no xylem vessel crossed the grafting union to more than 30 cm.

Magnetic resonance imaging measurements were conducted on four plants that were dark acclimated for ~2 h in order to maximize leaf water content. The dehydration occurred under dark conditions inside the MRI bore and was similar to the bench top dehydration as described by Choat *et al.* (2010). The imaged area was approximately 60 cm above the cut end and 50 cm (three–six internodes) above the grafting point, while the stem apex was still intact. The petiole and a reference tube with a 10 mM $Ni(NO_3)_2$ solution were fixed parallel to the stem by means of parafilm and subsequently enclosed in a 5 mm openable radiofrequency (RF) coil (Fig. 1a,d). Four leaves were enclosed in plastic bags and later used to measure Ψ_x. The rootstock was cut under water and the vine transferred into the MRI setup, while at all times keeping the cut end of the rootstock submerged in a 50 mL tube filled with water. The first image in the measurement series was acquired with the cut end still submerged under water and at xylem pressures no lower than −0.3 MPa, as was verified by measurements obtained

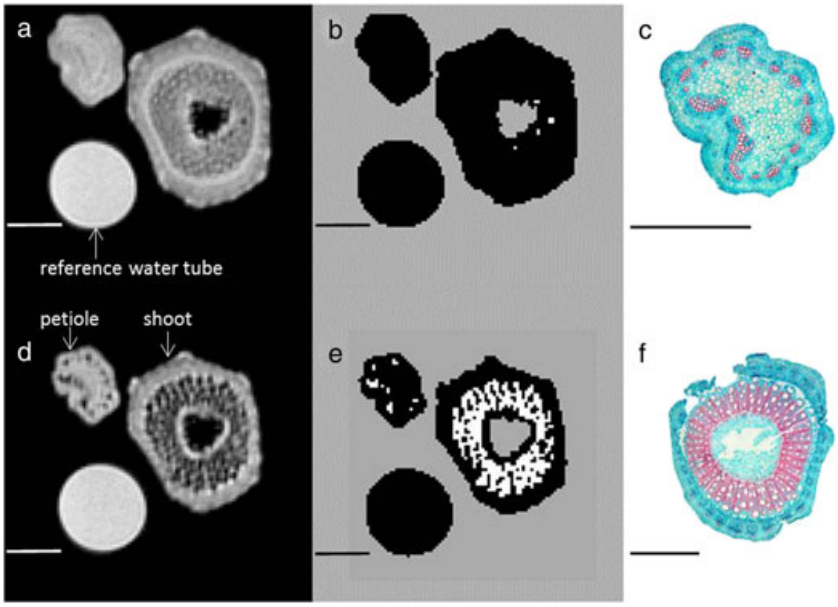

Figure 1. Assessment of embolism degree. Binary transformation was applied to all magnetic resonance images to dichotomously distinguish between conductive (black) or non-conductive (white) pixels. The percent of embolism of each image was calculated after normalization to the number of pixels at full conductivity (a,b $pix_{initial}$) and the number of pixels at full embolism (pix_{max}). Pix_{max} was validated by comparison with xylem area (in red) derived from microscopic cross-section images of petioles (c) and stem (f). The lines at the bottom left of all images represent 1 mm.

immediately after imaging. After acquiring the first image, the cut end of the vine was exposed to air by sucking the water out of the 50 mL tube from outside the imager. In this way, the vines were allowed to commence drying, without having to remove the vine from the closed cylindrical bore of the magnet and without causing movement of the sample. All subsequent images were taken while the vines were drying inside the MRI under continuous darkness at a temperature of 19 °C. Three of the four vines were dried for a period of between 12 and 16 h, ultimately reaching an average Ψ_x of −1.6 MPa. The fourth vine was left to dry in the MRI for a period of 40 h, reaching a Ψ_x of −1.94 MPa. In the latter case, Ψ_x was extrapolated from the relative petiole water content (as described in the following).

Magnetic resonance imaging

Magnetic resonance imaging was carried out using a superconducting, vertical bore 4.7 T Varian VNMRS MRI system (Varian, Palo Alto, CA, USA) fitted with a 300 mT/m gradient set with an inner diameter of 205 cm and a custom-built openable four-turn solenoidal RF coil of 5 mm in diameter. The RF coil was mounted at an angle of 45° with respect to the vertical main magnetic field (B0). Carr–Purcell–Meiboom–Gill amplitude-T_2 measurements were performed using the following settings: field of view (FOV), depending on object size, between 8 × 8 and 12 × 12 mm; slice thickness: 2 mm; matrix size: 128 × 128; number of averages: 2; echo time: 4 ms; number of echos: 32; repetition time: 5 s; total scan time per image: 25 m; and spectral width: 50 kHz. The acquired MRI data sets were processed using fitting routines written in IDL software (Research Systems Inc., Boulder, CO, USA). The data sets were fitted on a per pixel basis using a monoexponential decay function (van der Weerd *et al.* 2000), which yielded quantitative maps of amplitude and T_2 (Donker *et al.* 1997; Edzes, Van Dusschoten & Van As 1998). In the current study, only the resulting amplitude maps are shown.

All imaged petioles were later fixed in 70% ethanol and were embedded and sectioned following the methods of David-Schwartz *et al.* (2013). Xylem vessel diameter was analysed using ImageJ (Abramoff *et al.* 2004).

Xylem pressure (Ψ_x)

Measuring Ψ_x continuously is never trivial, but even more so inside an MRI scanner where the strong magnetic field prohibits the use of magnetic materials. To overcome the problem, we combined the pressure bomb method with the MRI capability to accurately measure water content in order to create a model linking the two. In four leaves per plant, Ψ_x was measured using a pressure bomb (Soil Moisture Equipment Corp., USA) according to the procedure described by Scholander *et al.* (1964). The measurements were taken before emptying the 50 mL tube (~ − 0.3 MPa), 25 min after drying (~ − 0.65 MPa), 100 min after drying (~ − 1.2 MPa) and 12–16 h after drying (~ − 1.6 Mpa). Measurements were performed on fully expanded leaves that were bagged (enclosed in plastic bags) for at least 30 min. Each leaf was excised from the stem using a sharp blade and then placed into the pressure chamber with the petiole protruding from the chamber lid. The chamber was pressurized using a pressurized nitrogen tank, and Ψ_x was recorded when the initial xylem sap was observed emerging from the cut end of the petiole.

The Ψ_x for all other MRI samples, apart from the four measurement points that were carried out as described earlier, was derived from a modification of the pressure-volume model (Turner 1988) applied to the petiole (Fig. 2). This model describes the relation between the cell's water content and water potential allowing the conversion of one to the other. We assumed that such a model would be more powerful applied to the petiole (rather than the stem) because of its composition of larger portion of parenchyma cells (Fig. 1c). The water content of each petiole was quantified using ImageJ (Abramoff *et al.* 2004) as the sum of the amplitudes of all its pixels normalized to the sum of all the pixels of the H_2O reference tube. Assuming that dark acclimated well-watered plants are close to 100% relative water content, the petiole's water content of each image was normalized to that of the first image. The third and fourth pressure bomb Ψ_x measurements (at ~ −1.2 and −1.6 MPa) were taken after wilting had occurred; their relative water content was subsequently linearly regressed with $1/\text{-}\Psi_x$ to model the osmotic modulus (Fig. 2; $R^2 = 0.92$).

Quantification of the degree of embolism formation

To be able to fit the stem together with an intact petiole and a reference tube in the FOV of the MRI scanner, a large FOV by necessity was chosen. This limited the spatial resolution that could be obtained to a pixel size of $40 \times 40\,\mu$m, which is larger than most vessels of the petioles (Hochberg *et al.* 2015). This precluded a straightforward embolism evaluation based on vessel count as demonstrated before (Choat *et al.* 2010; Holbrook *et al.* 2001). To overcome this problem, we had to determine embolism based on a per pixel basis, with the assumption that a pixel within the xylem area that changed from water-filled to air-filled had embolized and was non-functional. We assessed the degree of embolism through binary transformation using ImageJ (Abràmoff, Magalhães & Ram 2004). Binary transformation was used to assure that parenchyma cells would not be counted as embolism. Because the values of the parenchyma cells were much closer to the values of conductive xylem vessels than to those of empty xylem vessels, binary transformation always tagged them as conductive tissue. The organs shrinkage during dehydration was accounted for by modifying the analysed area to match the boundaries of the petiole or stem. Zero value pixels (marked in white in Fig. 1b,e) were counted and assumed to be embolized (pix_{emb}). The percent of embolism formation ($\%_{emb}$) was calculated as

$$\%\text{emb} = 100 \times \frac{\text{pix}_{\text{emb}} - \text{pix}_{\text{initial}}}{\text{pix}_{\text{max}} - \text{pix}_{\text{initial}}} \quad (1)$$

$pix_{initial}$ is the number of zero value pixels in the first image, and pix_{max} is the number of zero value pixels at 100% embolism inflicted by cutting the vessels open (Fig. 1d,e). The normalization to $pix_{initial}$ means that $\%_{emb}$ represents the appearance of new emboli but does not account for emboli that were already present before the start of the experiment (this, in contrast to the microCT embolism quantification method – described in the following). The two are probably similar but not identical because even under a well-watered condition (as the plants were grown), a certain degree of embolism (<10% of the total vessel population) is expected (microCT results in Fig. 5). The normalization to pix_{max} suggests that any effect that was not accounted for by the binary transformation was normalized, as it was probably also present in the last image.

To quantify pix_{max}, both the stem and petioles were cut directly under the coil, less than 1 cm beneath the imaged tissue, at the end of the dry down experiment. To verify that indeed the majority of vessels were longer than 1 cm and would therefore be embolized when cut under tension, we performed the following test. Short stem and petiole segments (5 cm) were flushed of all native embolism with membrane filtered distilled water (1 min, 150 kPa). The same segments, now free of emboli, were perfused with air at high pressure (200 kPa) in order to embolize all the open xylem vessels. The segments were divided under water with a sharp razor blade into two smaller (1 cm and 4 cm) segments, 1 cm away from the pressurized end. The PLC of both segments was evaluated using the Xyle'm apparatus (Xylem Embolism metre, Instructec, Montigny-les-Cormeilles, France) as described by Zufferey *et al.* (2011). In the 4 cm segment, 93.4% and 100% of the conductance of petioles and stems, respectively, was lost, indicating similar percentage of conducting area is open 1 cm away from a random cut.

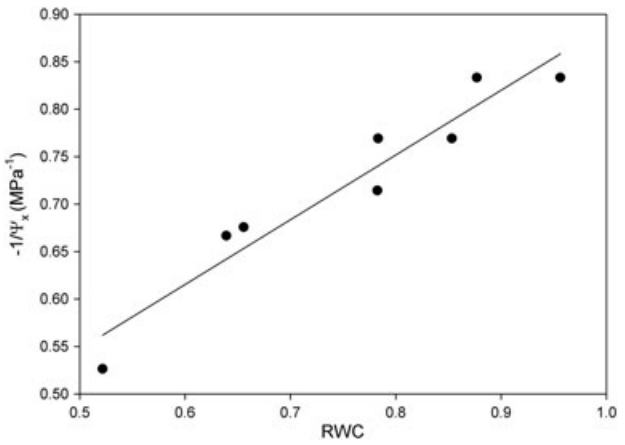

Figure 2. Relation between the petiole relative water content (RWC) and the xylem water potential (Ψx). To determine the Ψx, the linear regression below turgor loss point was used as suggested by Turner (1988).

Microcomputed tomography imaging

The xylem pressure in the stem was measured on bagged leaves with a Scholander Pressure Chamber (Soil Moisture Co., Santa Barbara, CA, USA), ~10–40 min before scanning each sample. Intact plants were prepared for scanning by carefully placing the axis of a petiole against the stem internode that it subtended, and these were held together with Kapton® tape (DuPont, Wilmington, DE, USA). The petiole and stem were scanned simultaneously and were located towards the base of each plant.

Imaging was conducted following the methods described by McElrone *et al.* (2012). The scans took approximately 6 min to complete using the continuous tomography setting at 20 keV at the Lawrence Berkeley National Laboratory Advanced Light Source, beamline 8.3.2. A 2× lens was utilized to produce images with a voxel resolution of 3.19 μm. Images were then reconstructed using Octopus 8.3 software (Institute for Nuclear Sciences, University of Ghent, Belgium) and analysed with ImageJ software (Abramoff *et al.* 2004) to count water-filled and embolized vessels. The high spatial resolution allowed the identification of individual vessels. The degree of embolism was quantified by dividing the number of embolized vessels by the total number of vessels.

Statistical analysis

In the MRI experiment, apart from the first five images, where dehydration was very fast, all images of the same vine in 0.1 MPa intervals were averaged, both in their Ψ_x and $\%_{emb}$. Values were averaged between the four replicated vines (n = 4) and compared in a *T*-test with the matching value of the other organ (petioles versus stems). To evaluate $\Psi_{50\%}$, sigmoidal curve fitting was performed using SigmaPlot 11 by adjusting $\%_{emb}$ versus Ψ_x as follows:

$$\%\text{emb} = \frac{100}{1 + e^{a(\psi_x - \psi_{50\%})}} \quad (2)$$

The slope (s) at the inflexion point was calculated as

$$s = a \times 25 \quad (3)$$

The averages acquired in the microCT experiment were compared with a *T*-test.

RESULTS

Magnetic resonance imaging was used to continuously and non-invasively measure the appearance of emboli in the stem and petiole of plants that were allowed to dry down (Fig. 3; also see Supporting Information time-lapse animation S1). Embolism formation was almost negligible for both organs in the first 100 min of dehydration, as the Ψ_x of the vines dropped from −0.3 to −1.2 MPa. Significant embolism formation was not noticed in either organ until values lower than −1.2 MPa were reached. Significant differences ($P < 0.01$) in the $\%_{emb}$ between stems and petioles were measured at all pressures less than and equal to −1.3 MPa. The quantification of $\%_{emb}$ resulted in two significant ($P < 0.01$ for 'a' and $\Psi_{50\%}$) sigmoidal vulnerability curves for the stems and petioles (Fig. 4). $\Psi_{50\%}$ was 0.37 MPa lower (more negative) in the stems (−1.9 MPa) than in the petioles (−1.54 MPa). The slope at the inflexion point of the petiole trace (159%/MPa, $P < 0.001$) was nearly twice as large as that of the stems (87%/MPa, $P < 0.001$) once embolism started to occur, further confirming the larger vulnerability of the petioles. In the stem, the larger vessels allowed the continuous visualization of the spatial pattern of embolism formation.

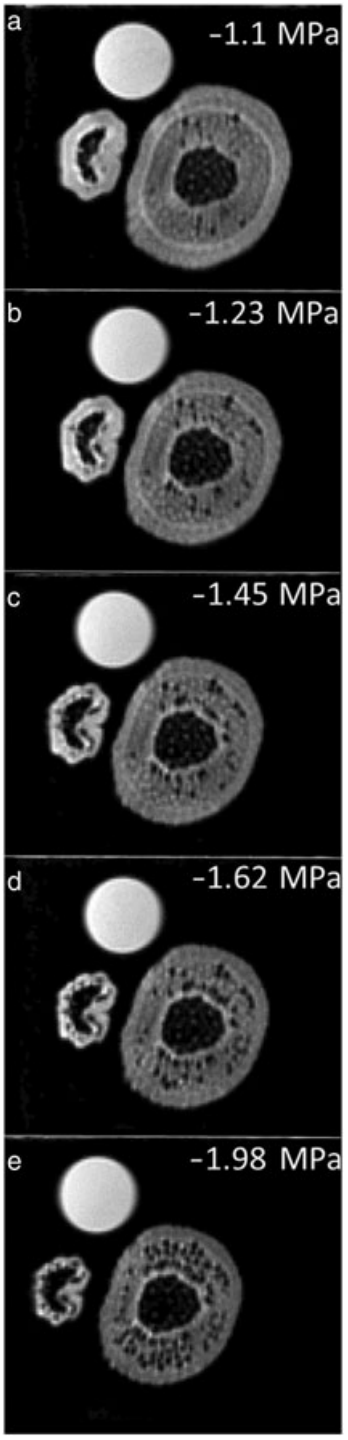

Figure 3. Five representative magnetic resonance images acquired during the vines dehydration and their correspondent xylem water potential. The petiole was paralleled to the stem and to a reference water tube.

The microCT imaging experiment confirmed the existence of the aforementioned vulnerability differences. The petioles exhibited a much larger degree of embolism than the stems at a similar Ψ_x (Fig. 5). In fact, the MicroCT results suggest an even larger difference between the degree of embolism of petioles and stems when compared with MRI results. The high

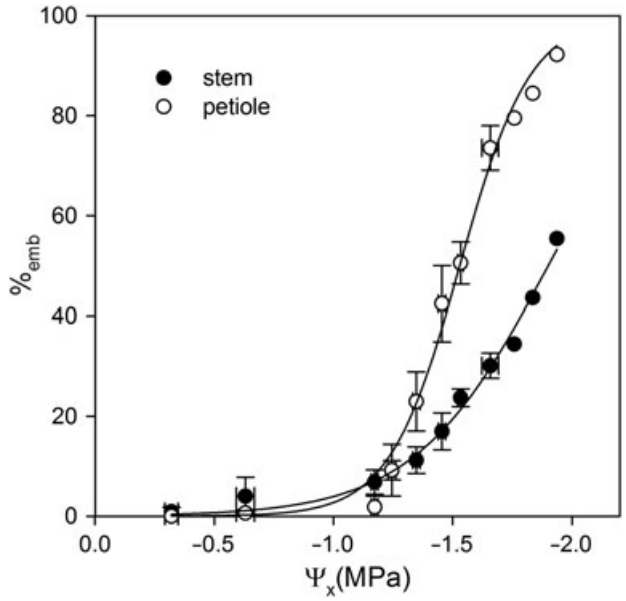

Figure 4. Vulnerability curves of stems (closed symbols) and petioles (open symbols) - sigmoidal fitting between the percent of embolized area (%emb) and the shoot water potential (Ψx). Data represent averages ± SE ($n = 4$).

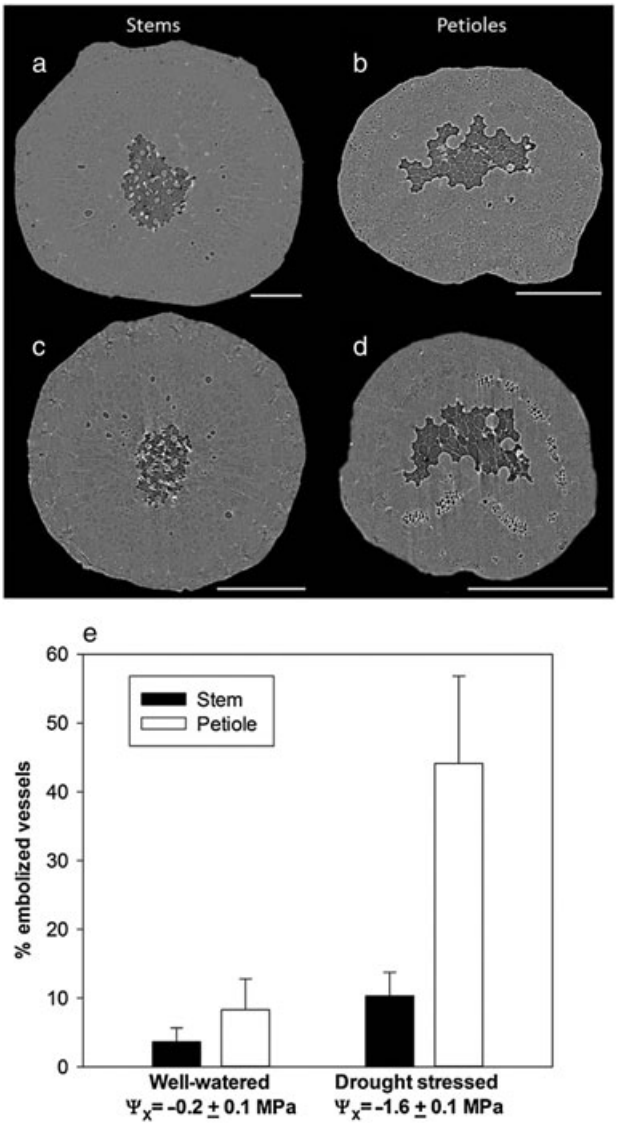

Figure 5. Representative transverse microcomputed tomography images of grapevine shoots and petioles (a–d) and the average degree of embolism (e). Images a and b were taken from the same plant (shoots and petiole, respectively), and images c and d were taken on another plant (shoot and petiole, respectively). Microcomputed tomography images a and b were taken on a well-watered vine ($\Psi_x = -0.3$ MPa), while c and d were taken on a drought-stressed vine ($\Psi_x = -1.5$ MPa). % embolized vessels for the four samples were a = 5.7, b = 3.8, c = 8.4 and d = 56.3. Scale bars located to the bottom right of each image represent 500 μm. The mean % of embolized vessels for stems and petioles of well-watered plants and drought-stressed plants were compared (e). Bars represent the mean SE $n = 4$.

spatial resolution of microCT makes it possible to spatially resolve and count individual vessels. It could thus be determined that at a Ψ_x of −0.2 MPa, both organs had very little embolized vessels (3–9% of vessels embolized). At −1.6 MPa in the petioles, 45% of the vessels were embolized, whereas in the stems on average, only 12% of the vessels were embolized.

DISCUSSION

Our results provide the first non-invasive observations of the hydraulic segmentation phenomenon *in vivo* and indicate that in intact Syrah plants under water deficit, petioles lose conductivity at less negative Ψ_x than stems (Fig. 3; Supporting Information time-lapse animation S1). These observations of hydraulic segmentation in *V vinifera* agree with previous measurements in deciduous plants (Tyree *et al.* 1993; Tsuda & Tyree 1997; Choat *et al.* 2005; Lovisolo *et al.* 2008), giving further support to the hypothesis proposed by Tyree & Ewers (1991) that this strategy may be common in woody, deciduous plants. Our methods also provided a unique opportunity to simultaneously study the functional status of two hydraulically linked organs and to then generate vulnerability curves to predict their respective loss of hydraulic conductivity.

Greater embolism resistance is often associated with smaller vessel diameters, as they are likely to have a lower surface area and fewer intervessel pits compared with larger diameter vessels (Wheeler *et al.* 2005). The average vessel diameter of the stem (25.44 ± 1.09 μm) is significantly larger than that of the petiole (9.95 ± 0.53 μm), and the stem's larger diameter vessels should, theoretically, be more vulnerable to embolism formation and spread. Our data suggest a different origin for the differences in embolism resistance. As the primary xylem is more sensitive to embolism than the secondary xylem, the larger primary/secondary xylem ratio in petioles (Choat *et al.* 2005) could, in part, lead to the differences in embolism vulnerability reported here. Additionally, there may be other xylem network properties (e.g. pit morphology, pit membrane thickness, vessel ending frequency, xylem/tracheid proportion and conduit redundancy; Jansen, Choat & Pletsers 2009; Guet *et al.* 2015) that were not considered in this study and may play an important role in the differences in cavitation resistance between the two tissue types.

Measurements of Ψ_x were conducted through leaf bagging, thereby stopping leaf transpiration and allowing the xylem pressure of the leaf to equilibrate with that of the stem. The Ψ_x values reported here thus represent an average of the Ψ_x of both the petiole and the stem. Because of the equilibration between the two organs, we were not able to determine the Ψ_x gradient between the stem and petiole and thus could not determine whether the differences in cavitation resistance between the two organs are a product of vulnerability to embolism (Tyree & Ewers 1991) or hydraulic segmentation (where Ψ_x is expected to be more negative in distal organs; Zimmermann 1983). However, the contribution of hydraulic segmentation to these observations is questioned as it will require high transpiration rates, which are not likely to occur in the dark conditions under which the MRI experiment took place. The phenomenon is more likely to occur when plants were illuminated, such as during the microCT experiment, which might explain the larger differences that were observed as compared with MRI. Under field conditions, pressure differences of 0.2 MPa between grapevine leaves and stems are commonly found (Williams & Araujo 2002), and thus, hydraulic segmentation may increase the differences in embolism between the two organs.

Zwieniecki *et al.* (2013) showed that reliable vulnerability curves can be generated using MRI, even in cases where the spatial resolution does not allow the individual vessels to be fully resolved. As Zwieniecki *et al.* (2013) used an air injection method to induce embolism, water loss from non-vessel cells was minor, allowing the quantification of PLC on the basis of pixel brightness. This was not the case during the long dehydration we performed in the current study, which will have resulted in significant water loss from parenchyma and fibre cells and thus in an equally significant loss in MRI signal amplitude. We circumvent this problem by means of the binary image transformation approach, which enabled us to detect the occurrence of emboli, irrespective of the water status of the surrounding tissue. The vulnerability curves obtained by means of MRI and microCT were consistent with each other and in good agreement with the data in the literature. The stem vulnerability curves were similar to the ones published by Choat *et al.* (2010), who employed high-resolution MRI as well as traditional bench dehydration of long stems to acquire their PLC values. In addition, Brodersen *et al.* (2013) reported a vulnerability curve for small *V. vinifera* (cv Chardonnay) stems with microCT that agree well with the MRI curves presented here (Fig. 4).

At Ψ_x of down to −1.1 MPa, we observed the formation of only a negligible number of emboli ($\%_{emb}$ close to 0; Fig. 4) in both stem and petiole. These findings, which are the first *in vivo* visualizations of embolism in grapevine petiole, strongly contrast with previous invasive measurements. Zufferey *et al.* (2011) and Lovisolo *et al.* (2008) already found a substantial degree of PLC (40%) in petioles of grapevines at Ψ_x above −1 MPa. Tombesi *et al.* (2014) measured $\Psi_{50\%}$ values that were not only slightly lower (−1.08 or −1.25 MPa for Montepulciano and Sangiovese cultivars, respectively) but also already measured about 30% PLC at a high Ψ_x of −0.5 MPa. These differences suggest the existence of a discrepancy between invasive and non-invasive methods of embolism evaluation. The difference cannot be attributed to the methodical differences in calculating PLC and $\%_{emb}$ (percentage loss of conductivity versus % of vessels embolized), as such a distinction cannot be claimed when $\%_{emb}$ is zero. A more likely explanation was provided by Wheeler *et al.* (2013). These authors showed that cutting the xylem under tension may artificially introduce emboli into the xylem and result in apparent higher degree of PLC. Evidence suggesting that the studies by Lovisolo *et al.* (2008) and Zufferey *et al.* (2011) may have suffered from this artefact is provided by their observation that most PLC disappeared as soon as Ψ_x was increased when evening approached. Nonetheless, because the Wheeler *et al.* (2013) findings cannot be generalized to be valid for all species (Wheeler *et al.* 2013; Venturas *et al.* 2015), and because concerns about potential fast xylem refilling were raised (Trifilo *et al.* 2014), there still is a need to more closely test for the existence of a cutting artefact in grapevine petioles. Alternatively, the high PLC found at Ψ_x could also have resulted from emboli that already had been introduced before, for example during episodes when Ψ_x was more negative, and were never completely removed from the system. Our data thus suggest that in grapevine, the formation of emboli in the stem and petiole at high Ψ_x is more rare an occurrence than previously presumed.

It has been hypothesized that emboli could play a role in the regulation of transpiration. Zufferey *et al.* (2011) suggested that vulnerability segmentation could be an efficient mechanism for grapevines to regulate stomatal opening. The xylem vessels in the petioles could act as 'hydraulic fuses', and their embolization would thus limit leaf transpiration. However, it seems that embolism formation in stem and petioles of grapevines does not occur until Ψ_x reaches values that are much more negative than the ones inducing stomatal closure. Even more so, the hypothesis that the induction of embolism could act as a signal for stomata closure (Nardini & Salleo 2000) is not supported by our findings. For any kind of regulation to be associated with the appearance of emboli, the emboli should precede the proposed effect. Stomata conductance is normally reduced by half (compared with well-watered conditions) when water potentials are reduced to −0.75 MPa (Zufferey *et al.* 2011; Tombesi *et al.* 2014; Hochberg *et al.* 2013). In the current study, at such Ψ_x, we were not able to detect any embolism in the petiole or in the stem (Fig. 4). Similarly, the reduction of leaf and vine hydraulic conductance normally appear shortly after dehydration starts (Zufferey *et al.* 2011); therefore, the involvement of stem or petiole embolism is not likely. Rather, it reinforces the view that vulnerability segmentation serves as a second line of defence in the event that leaf conductance declines and stomata regulation fails. Only under severe stress, the petioles would experience significant embolism induction, thus limiting further water loss and most importantly, assuring the preservation of the functional integrity of the xylem in the stem. This view is corroborated by the observation that grapevines tend to shed their leaves under severe water stress, yet often are able to recover rapidly upon irrigation. It should be noted that this does not necessarily mean that embolism did not play a role at all. Embolism formation in the leaf blade may precede embolism formation in the petioles and thus reduce leaf conductance and limit transpiration (Johnson *et al.* 2012; Nolf *et al.* 2015).

In conclusion, in the current study, we present the first *in vivo* observations of vulnerability segmentation in intact plants. Under water deficit, xylem vessels in the petioles of grapevines on average embolize before vessels in the stems do. Our vulnerability curves suggest that embolism-induced xylem failure in grapevine may be a much rarer occurrence than is commonly assumed.

ACKNOWLEDGMENTS

The authors wish to express their gratitude to Bernd Gruber, Manfred Stoll and Hans R Schulz from the Hochschule Geisenheim University for their help with plant material and equipment. We thank dr. Dagmar van Dusschoten for his help using the 4.7 T MR imager at the IBG-2 Plant Sciences Institute and for making the microcoil setup available. We thank D. Parkinson and A. MacDowell for their assistance at the Lawrence Berkeley National Laboratory Advanced Light Source beamline 8.3.2 microtomography facility and I.F. Cuneo for assistance with image capture/analysis. The MRI analysis in the study was conducted as part of a short-term scientific mission in the COST Action STReESS: Studying Tree Responses to extreme Events: a SynthesiS (Reference number: FP1106170414-039538). This work was supported by the US Department of Agriculture-Agricultural Research Service Current Research Information System funding (research project no. 5306–21220–004–00). The Advanced Light Source is supported by the Director, Office of Science, Office of Basic Energy Sciences, of the US Department of Energy (contract no. DE–AC02–05CH11231). U.H. was supported by the Chateau Briand fellowship and C.A. by the CAPES/Brazil scholarship.

REFERENCES

Abràmoff M.D., Magalhães P.J. & Ram S.J. (2004) Image processing with ImageJ. *Biophotonics International* **11**, 36–42.

Alsina M., De Herralde F., Aranda X., Save R. & Biel C. (2007) Water relations and vulnerability to embolism are not related: experiments with eight grapevine cultivars. *Vitis* **46**, 1–6.

Brodersen C.R., McElrone A.J., Choat B., Lee E.F., Shackel K.A. & Matthews M.A. (2013) *In vivo* visualizations of drought-induced embolism spread in *Vitis vinifera*. *Plant Physiology* **161**, 1820–1829.

Brodersen C.R., McElrone A.J., Choat B., Matthews M.A. & Shackel K.A. (2010) The dynamics of embolism repair in xylem: *in vivo* visualizations using high-resolution computed tomography. *Plant Physiology* **154**, 1088–1095.

Choat B., Drayton W.M., Brodersen C., Matthews M.A., Shackel K.A., Wada H. & Mcelrone A.J. (2010) Measurement of vulnerability to water stress-induced cavitation in grapevine: a comparison of four techniques applied to a long-vesseled species. *Plant, Cell & Environment* **33**, 1502–1512.

Choat B., Lahr E.C., Melcher P.J., Zwieniecki M.A. & Holbrook N.M. (2005) The spatial pattern of air seeding thresholds in mature sugar maple trees. *Plant, Cell & Environment* **28**, 1082–1089.

Cochard H., Bréda N., Granier A. & Aussenac G. (1992) Vulnerability to air embolism of three European oak species (*Quercus petraea* (matt) liebl, Q pubescens willd, Q robur L). **49**, 225–233.

Cochard H., Delzon S. & Badel E. (2015) X-ray microtomography (micro-CT): a reference technology for high-resolution quantification of xylem embolism in trees. *Plant, Cell & Environment* **38**, 201–206.

David-Schwartz R., Borovsky Y., Zemach H. & Paran I. (2013) CaHAM is autoregulated and regulates CaSTM expression and is required for shoot apical meristem organization in pepper. *Plant Science* **203**, 8–16.

Dixon H. (1914) Transpiration and the ascent of sap in Plants MacMillan.

Donker H., Van As H., Snijder H. & Edzes H. (1997) Quantitative1H-NMR imaging of water in white button mushrooms (*Agaricus bisporus*). *Magnetic Resonance Imaging* **15**, 113–121.

Edzes H.T., Van Dusschoten D. & Van As H. (1998) Quantitative T2 imaging of plant tissues by means of multi-echo MRI microscopy. *Magnetic Resonance Imaging* **16**, 185–196.

Ewers F.W. & Fisher J.B. (1989) Techniques for measuring vessel lengths and diameters in stems of woody plants. *American Journal of Botany* 645–656.

Guet J., Fichot R., Ledee C., Laurans F., Cochard H., Delzon S., Bastien C. & Brignolas F. (2015) Stem xylem resistance to cavitation is related to xylem structure but not to growth and water-use efficiency at the within-population level in *Populus nigra* L. *Journal of Experimental Botany*. DOI:10.1093/jxb/erv232.

Hochberg U., Degu A., Fait A. & Rachmilevitch S. (2013) Near isohydric grapevine cultivar displays higher photosynthetic efficiency and photorespiration rates under drought stress as compared with near anisohydric grapevine cultivar. *Physiologia Plantarum* **147**, 443–453.

Hochberg U., Degu A., Gendler T., Fait A. & Rachmilevitch S. (2015) The variability in the xylem architecture of grapevine petiole and its contribution to hydraulic differences. *Functional Plant Biology* **42**, 357–365.

Holbrook N.M., Ahrens E.T., Burns M.J. & Zwieniecki M.A. (2001) *In vivo* observation of cavitation and embolism repair using magnetic resonance imaging. *Plant Physiology* **126**, 27–31.

Jansen S., Choat B. & Pletsers A. (2009) Morphological variation of intervessel pit membranes and implications to xylem function in angiosperms. *American Journal of Botany* **96**, 409–419.

Johnson D.M., McCulloh K.A., Woodruff D.R. & Meinzer F.C. (2012) Evidence for xylem embolism as a primary factor in dehydration-induced declines in leaf hydraulic conductance. *Plant, Cell & Environment* **35**, 760–769.

Knipfer T., Eustis A., Brodersen C., Walker A.M. & McElrone A.J. (2014) Grapevine species from varied native habitats exhibit differences in embolism formation/repair associated with leaf gas exchange and root pressure. *Plant, Cell & Environment* **38**, 1503–1513.

Lovisolo C., Perrone I., Hartung W. & Schubert A. (2008) An abscisic acid-related reduced transpiration promotes gradual embolism repair when grapevines are rehydrated after drought. *New Phytologist* **180**, 642–651.

McElrone A., Brodersen C., Alsina M., Drayton W., Matthews M., Shackel K., … Choat B. (2012) Centrifuge technique consistently overestimates vulnerability to water stress-induced cavitation in grapevines as confirmed with high-resolution computed tomography. *New Phytologist* **196**, 661–665.

Nardini A. & Salleo S. (2000) Limitation of stomatal conductance by hydraulic traits: sensing or preventing xylem cavitation? *Trees* **15**, 14–24.

Nolf M., Creek D., Duursma R., Holtum J., Mayr S. & Choat B. (2015) Stem and leaf hydraulic properties are finely coordinated in three tropical rainforest tree species. *Plant, Cell & Environment*. DOI:10.1111/pce.12581.

Scheenen T.W., Vergeldt F.J., Heemskerk A.M. & Van As H. (2007) Intact plant magnetic resonance imaging to study dynamics in long-distance sap flow and flow-conducting surface area. *Plant Physiology* **144**, 1157–1165.

Scholander P.F., Hammel H.T., Hemmingsen E.A. & Bradstreet E.D. (1964) Hydrostatic pressure and osmotic potential in leaves of mangroves and some other plants. *Proceedings of the National Academy of Sciences of the United States of America* **52**, 119–125.

Schultz H. (2003) Differences in hydraulic architecture account for near-isohydric and anisohydric behaviour of two field-grown *Vitis vinifera* L. cultivars during drought. *Plant, Cell & Environment* **26**, 1393–1405.

Tombesi S., Nardini A., Farinelli D. & Palliotti A. (2014) Relationships between stomatal behavior, xylem vulnerability to cavitation and leaf water relations in two cultivars of *Vitis vinifera*. *Physiologia Plantarum* **152**, 453–464.

Torres-Ruiz J.M., Jansen S., Choat B., McElrone A.J., Cochard H., Brodribb T.J., … Delzon S. (2015) Direct x-ray microtomography observation confirms the induction of embolism upon xylem cutting under tension. *Plant Physiology* **167**, 40–43.

Tsuda M. & Tyree M.T. (1997) Whole-plant hydraulic resistance and vulnerability segmentation in *Acer saccharinum*. *Tree Physiology* **17**, 351–357.

Turner N.C. (1988) Measurement of plant water status by the pressure chamber technique. *Irrigation Science* **9**, 289–308.

Tyree M.T. & Ewers F.W. (1991) The hydraulic architecture of trees and other woody plants. *New Phytologist* **119**, 345–360.

Tyree M.T. & Sperry J.S. (1989) Vulnerability of xylem to cavitation and embolism. *Annual Review of Plant Biology* **40**, 19–36.

Tyree M., Cochard H., Cruiziat P., Sinclair B. & Ameglio T. (1993) Drought-induced leaf shedding in walnut: evidence for vulnerability segmentation. *Plant, Cell & Environment* **16**, 879–882.

van der Weerd L., Vergeldt F.J., Adrie de Jager P. & Van As H. (2000) Evaluation of algorithms for analysis of NMR relaxation decay curves. *Magnetic Resonance Imaging* **18**, 1151–1158.

Venturas M.D., MacKinnon E.D., Jacobsen A.L. & Pratt R.B. (2015) Excising stem samples underwater at native tension does not induce xylem cavitation. *Plant, Cell & Environment* **38**, 1060–1068.

Wheeler J.K., Huggett B.A., Tofte A.N., Rockwell F.E. & Holbrook N.M. (2013) Cutting xylem under tension or supersaturated with gas can generate PLC and the appearance of rapid recovery from embolism. *Plant, Cell & Environment* **36**, 1938–1949.

Wheeler J.K., Sperry J.S., Hacke U.G. & Hoang N. (2005) Inter-vessel pitting and cavitation in woody rosaceae and other vesselled plants: a basis for a safety versus efficiency trade-off in xylem transport. *Plant, Cell & Environment* **28**, 800–812.

Williams L. & Araujo F. (2002) Correlations among predawn leaf, midday leaf, and midday stem water potential and their correlations with other measures of soil and plant water status in *Vitis vinifera*. *Journal of the American Society for Horticultural Science* **127**, 448–454.

Zimmermann M.H. (1983) The hydraulic architecture of plants. In Xylem Structure and the Ascent of Sap. pp. 66–82. Springer.

Zufferey V., Cochard H., Ameglio T., Spring J.L. & Viret O. (2011) Diurnal cycles of embolism formation and repair in petioles of grapevine (*Vitis vinifera* cv. chasselas). *Journal of Experimental Botany* **62**, 3885–3894.

Zwieniecki M.A., Melcher P.J. & Ahrens E.T. (2013) Analysis of spatial and temporal dynamics of xylem refilling in *Acer rubrum* L. using magnetic resonance imaging. *Frontiers in Plant Science* **4**, 265.

Received 26 September 2015; received in revised form 24 November 2015; accepted for publication 28 November 2015

SUPPORTING INFORMATION

Additional Supporting Information may be found in the online version of this article at the publisher's web-site.